

RESEARCH ARTICLE

Domain-size and top-height dependence in regional predictions for the Northeast Asia in spring

In-Sun Song¹ | Ui-Yong Byun² | Jinkyu Hong² | Sang-Hun Park²

¹Division of Polar Climate Sciences, Korea Polar Research Institute, Incheon, Korea

²Department of Atmospheric Sciences, Yonsei University, Seoul, Korea

Correspondence

J. Hong, Department of Atmospheric Sciences, Yonsei University, Seoul 03722, Korea.
Email: jhong@yonsei.ac.kr

Author Contribution

I.-S.S. and J.H. involved in data interpretation, experimental design, and manuscript preparation. U.-Y.B. involved in model simulation and modification. S.-H.P. involved in data interpretation.

Funding information

Korea Polar Research Institute, Grant/Award numbers: PE17020, PN17081; Korea Meteorological Administration, Grant/Award number: KMIPA2015-2063

For regional weather forecasts and climate predictions, it is important to determine the optimal domain size, location, and top height. A wide model domain can be chosen to avoid noises from lateral boundaries but this can include the Tibetan Plateau and areas of northern Manchuria to the Kamchatka Peninsula in Northeast Asia. This study shows that topographic regions around the Tibetan Plateau and warm pool areas over the Manchuria in an extended model domain may have harmful effects on the accuracy of short- to medium-range regional predictions on the downwind side in spring. The inaccuracy is related to model errors due to steep terrain regions in the Tibetan Plateau and cold bias in the lower stratosphere north of Manchuria. Well-designed spectral nudging over the eastern flank of the Tibetan Plateau and the use of a higher model top are found to improve regional predictions for Northeast Asia in spring by effectively eliminating errors associated with steep topography and temperature biases in the upper troposphere and lower stratosphere, respectively. Our findings suggest possible ways to mitigate biases due to steep mountains and upper-level processes in regional modeling. We discuss the role of our method in terms of uncertainties in regional weather forecasts and climate predictions.

KEYWORDS

domain size, model top, Northeast Asia, ozone, regional model, spectral nudging, troposphere–stratosphere

1 | INTRODUCTION

Regional models require initial and time-dependent lateral boundary conditions from global forecasts or analyses. Because regional modeling is carried out in limited areas, the evaluation of domain dependence to determine the optimal domain-related configuration has long been an important topic (e.g., Collin, Déqué, Radu, & Somot, 2010; Giorgi & Mearns, 1999; Jones, Murphy, & Noguer, 1995; Landman, Seth, & Camargo, 2005). Along lateral boundaries, there may exist dynamical inconsistency between global-scale data and prognostic variables in regional models used to simulate small-scale and high-frequency

motions. Spurious signals due to dynamical inconsistencies may propagate into the regional model domain and contaminate predictions (e.g., Leduc & Laprise, 2009; Park, Klemp, & Skamarock, 2014). Hence, the use of a larger horizontal domain has been recommended for better regional modeling (Warner, Peterson, & Treadon, 1997), although the actual effect may vary depending on cases (e.g., Vannitsem & Chomé, 2005).

For Northeast Asia, choosing a wide model domain may make the Tibetan Plateau (TP), Manchuria and the Kamchatka Peninsula (MK) included in the model domain. The TP can induce peculiar air flows due to strong radiative forcing related to its high elevation and vigorous dynamical

forcing in steep slope regions at the lee side and stagnation regions over the eastern flank at the Sichuan Basin (SB) (e.g., Jiang, Li, Zhao, & Koike, 2012; Shin & Lee, 2015; Tao & Ding, 1981; Wang & Orlanski, 1987). Numerical simulations of such unique flow structures are challenging, and inaccurate simulations may produce unreliable predictions for Northeast Asia (Zhang, Li, Fu, Liu, & Li, 2014, and references therein). One practical way to avoid this difficulty would be simply excluding the TP from the model domain. However, we consider the TP in this study to understand what characteristics of the TP can cause uncertainties in the predictions for Northeast Asia.

The inclusion of the MK region in the model domain may also affect predictions for Northeast Asia through model top boundary especially in winter and spring. The lower stratospheric flows associated with the longitudinally dependent Brewer–Dobson (BD) circulation (Demirhan Bari, Gabriel, Körnich, & Peters, 2013) produce warm layers over the MK region (Kozubek, Krizan, & Lastovicka, 2015; Šácha, Kuchař, Jacobi, & Pišcoft, 2015) in winter and spring. This warming correlates with the high concentration of ozone in the upper troposphere and lower stratosphere (UTLS) over the MK regions in these two seasons (Šácha *et al.*, 2015). This strong correlation is likely related to the downward branch of the BD circulation, although the spatial distribution of ozone may not always clearly explain the BD circulation (Butchart, 2014). However, regional models are often configured to simulate to altitudes just above the tropopause. In this study, we extend the model top height to the stratosphere to examine effects of such lower stratospheric processes on regional predictions.

This study focuses on understanding how steep topographic areas around the TP and warm pool regions in the UTLS over the MK region affect regional predictions for Northeast Asia in spring. In Section 2, model used in this study, domain configuration, and experiments are described. In Section 3, we discuss prediction errors due to the TP areas and the UTLS processes over the MK region through case simulations for April 2013. We then propose possible methods

to improve short- to medium-range regional predictions for Northeast Asia by showing how model errors due to a large horizontal domain and low model top height can be reduced. Summary and conclusions is given in the last section.

2 | MODEL AND EXPERIMENTS

The Weather Research and Forecasting (WRF) model (Skamarock *et al.*, 2008) version 3.6 is employed in this study. All numerical experiments are carried out with the same physics package. The essential components of the physics package are as follows: WRF double moment 6-class scheme (WDM6) for cloud microphysics, rapid radiative transfer scheme for general circulation models (RRTMG) for longwave and shortwave radiation, Yonsei University (YSU) scheme for the planetary boundary layer (YSU PBL), simple cloud-interactive radiation scheme, and National Centers for Environmental Prediction (NCEP)-Oregon State University-US Air Force-National Weather Service Office of Hydrologic Development (NOAH) land surface model (Lee & Hong, 2016, and references therein).

In this study, one-way nesting is used in a single-nested domain configuration (Figure 1). A 6-km horizontal resolution domain 2 centered on the Korean Peninsula is embedded in the 18-km resolution domain 1. Initial and lateral boundary conditions for domain 1 are generated using the 6-hourly European Centre for Medium-Range Weather Forecasts (ECMWF) Interim reanalyses ($0.75^\circ \times 0.75^\circ$). All simulations are also carried out using NCEP Global Forecast System (GFS) forecasts ($0.5^\circ \times 0.5^\circ$), but results driven by the ECMWF reanalyses are mainly shown in this study because the use of the GFS data does not lead to different conclusions.

Experiments in this study consist of sensitivity tests for different sizes and locations of domains 1 and 2, model top height, and spectral nudging. All experiments are described in Table 1. In the SD1 experiment, domain 1 only covers the Northeast Asia, but in the LD1, it is extended to include the TP, Siberia, and Indochinese Peninsula (Figure 1). In the LD1G experiment, spectral nudging (Miguez-Macho,

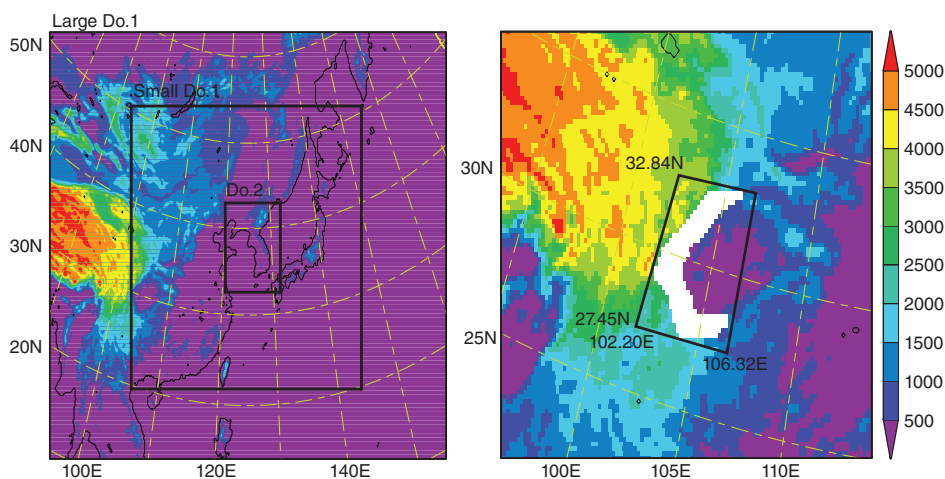


FIGURE 1 (Left) Domain configuration overlaid on model topography and (right) enlarged map around the Sichuan Basin. Spectral nudging is only applied to the C-shaped white area in the LD1G experiment. The C-shaped area is located within the region of 27.5° – 32.8° N and 102.2° – 106.3° E

TABLE 1 Descriptions of numerical experiments

Abbreviation	Description
SD1	Small domain 1. The TP and MK are excluded (Figure 1)
SD1W, SD1E, SD1S, SD1N	Same as SD1 except that the small domain 1 is displaced westward (SD1W), eastward (SD1E), southward (SD1S) and northward (SD1N) (Figure S1). Note that, SD1W only includes the eastern TP (Sichuan Basin)
LD1	Large domain 1. The eastern TP and MK are included (Figure 1)
LD1G	Same as LD1 except that spectral nudging is applied to the whole area of the large domain 1
LD1GB	Same as LD1G except that spectral nudging is applied to the lower layers (Figure S3) around the western boundaries of the Sichuan Basin
LD1GBT15	Same as LD1GB except that the model top is raised from 50 to 15 hPa
LD1GBT05	Same as LD1GBT15 except that the model top is raised to 5 hPa

Stenchikov, & Robock, 2004) is applied to horizontal wind (U and V), temperature (T), and perturbation geopotential (PH) at every grid point of the large domain 1. In the spectral nudging, the four model variables are nudged every physics time step towards the corresponding variables obtained from global data with large-scale structure in the computational rectangle (x - y) of domain 1. The large-scale structure is obtained using two-dimensional Fourier low-pass filtering for the large domain 1 with threshold wavenumbers of 9 and 7 in the x and y directions, respectively. As a result, global data with horizontal scales larger than approximately 800 km are used for spectral nudging. The nudging coefficient is set to 0.0006 s^{-1} . In the LD1GB

experiment, spectral nudging is only applied below about 300 hPa (Figure S3 in Supporting information) around the western boundaries of the SB regions where the topography is significantly steep (see the right panel of Figure 1) by forcing the spectral nudging terms at each grid point to be zero outside of the western boundary of the SB regions. In the LD1GBT15 and LD1GBT05 experiments, the model top is raised from 50 hPa to 15 hPa and 5 hPa, respectively, by inserting additional layers in the lower stratosphere and retaining the same vertical resolution ($\Delta z \approx 1.06 \text{ km}$) in the lower stratosphere. The number of default vertical layers is 31 when the model top is located at 50 hPa. The number of layers becomes 39 and 47 when the model top is raised to 15 and 5 hPa, respectively.

In this study, we consider six cases initialized at 0000 UTC on 3, 10, 17, and 24 April 2013, on 25 April 2013, and 12 April 2015. All sensitivity tests described in Table 1 are performed for each case. However, in the next section, we will present results mainly focusing on the first case (April 3, 2013) where the amount of observed precipitation within the small domain 1, in which prediction statistics are measured, was substantial compared with the other cases.

3 | RESULTS

3.1 | Analysis of prediction errors

Figure 2 demonstrates the time evolution of the geopotential height at 850 hPa in the LD1 and LD1G experiments and

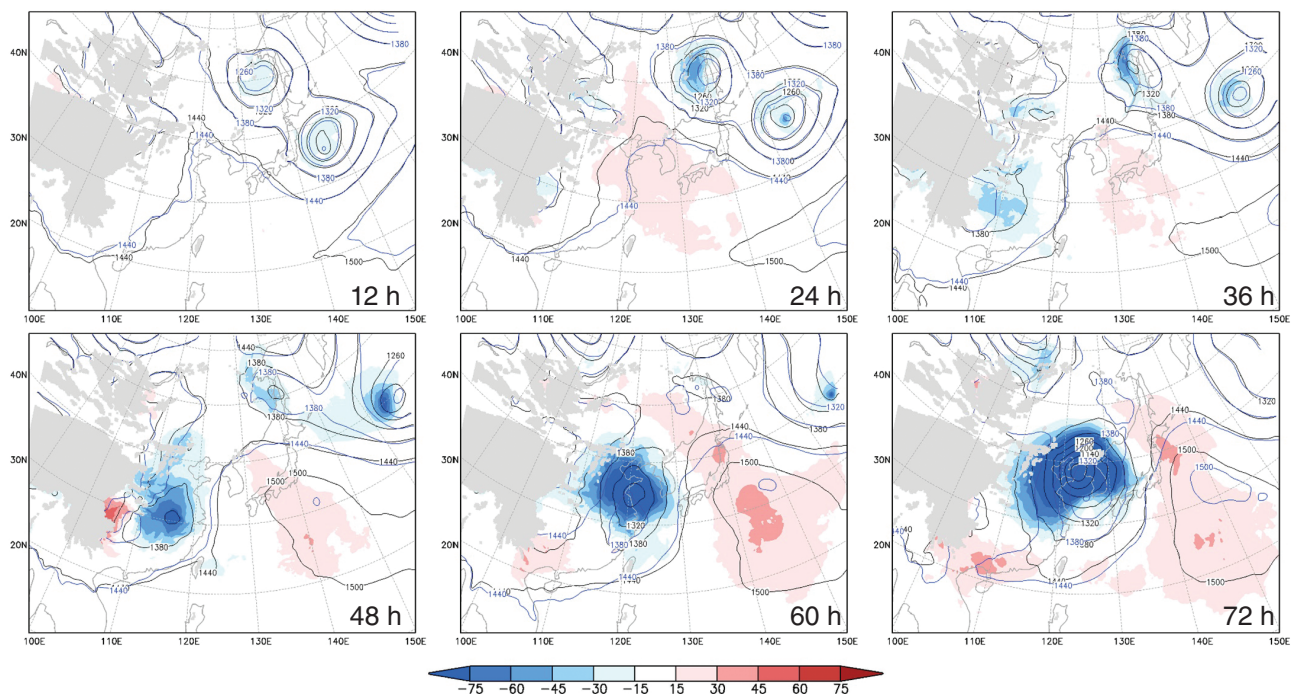


FIGURE 2 Geopotential heights (contour) at 850 hPa in the LD1 and LD1G experiments and the difference (shading) between the two simulations (LD1 - LD1G) at an interval of 12 hr from the 12-hr forecast time. The contours of the geopotential heights for the LD1 (LD1G) experiment is plotted in black (blue)

the difference (LD1 – LD1G) between the two simulations. In the LD1G experiment in which spectral nudging is applied every grid point, the spatial distribution and temporal evolution of field variables are almost similar to those of the ECMWF Interim reanalyses. The LD1 and LD1G experiments show small differences at the eastern flank of the TP at a 24-hr forecast time, but the differences rapidly grow after a 48-hr forecast time. The TP vortex is certainly a numerical artifact that did not actually occur during April 3–6, 2013. This spurious vortex is subsequently advected towards the Korean Peninsula and distorts the pattern of 24-hr accumulated precipitation in the domain 2 (0000 UTC on April 7 through 0000 UTC on April 8, Figure S7). Figure 2 also suggests that the prediction errors for Northeast Asia may originate from the SB areas. Furthermore, it is remarkable that similar prediction degradation in the small domain 1 when the small domain 1 includes the eastern flank of the TP as in the SD1W experiment (see Figures S1 and S2 for details).

Figure 3 shows the root-mean-square deviations (RMSDs) and correlation coefficients for the geopotential heights at 100 and 500 hPa, and sea-level pressure in all the experiments for April 3, 2013. The RMSDs and correlation coefficients are computed in the small domain 1. The

RMSDs in the LD1 experiment rapidly increase with time after about 36-hr (1.5-day) forecast time and generally exhibit the largest value among all experiments, which indicates that the prediction quality is the worst in the LD1 experiment in which the domain 1 includes the TP and MK region (Figure 1). It is also noticeable that the correlation coefficients at 500 hPa and sea-level pressure substantially drop after about 48-hr (2-day) forecast time in the LD1 experiment. It is likely that the abrupt reduction of the correlation coefficients after 48-hr forecast time is related to sudden and spurious amplification of TP vortices around the SB as shown in Figure 2.

In models that employ the terrain-following vertical coordinate, the pressure gradient force (PGF) may have significant errors around steep topographic regions such as the western boundary of the SB east of the TP (Messinger, 1982; Simmons & Burridge, 1981), although the numerical methods have been revised in a couple of studies to reduce PGF errors for idealized topographies (e.g., Good, Gadian, Lock, & Ross, 2014; Mahrer, 1984). In addition to PGF errors, uncertainties in the horizontal diffusion, topographic wind correction (Jiménez & Dudhia, 2012; Lee *et al.*, 2015), topographic shading effect (Ruiz-Arias, Pozo-Vázquez, Lara-Fanego, Santos-Alamillos, & Tovar-Pescador,

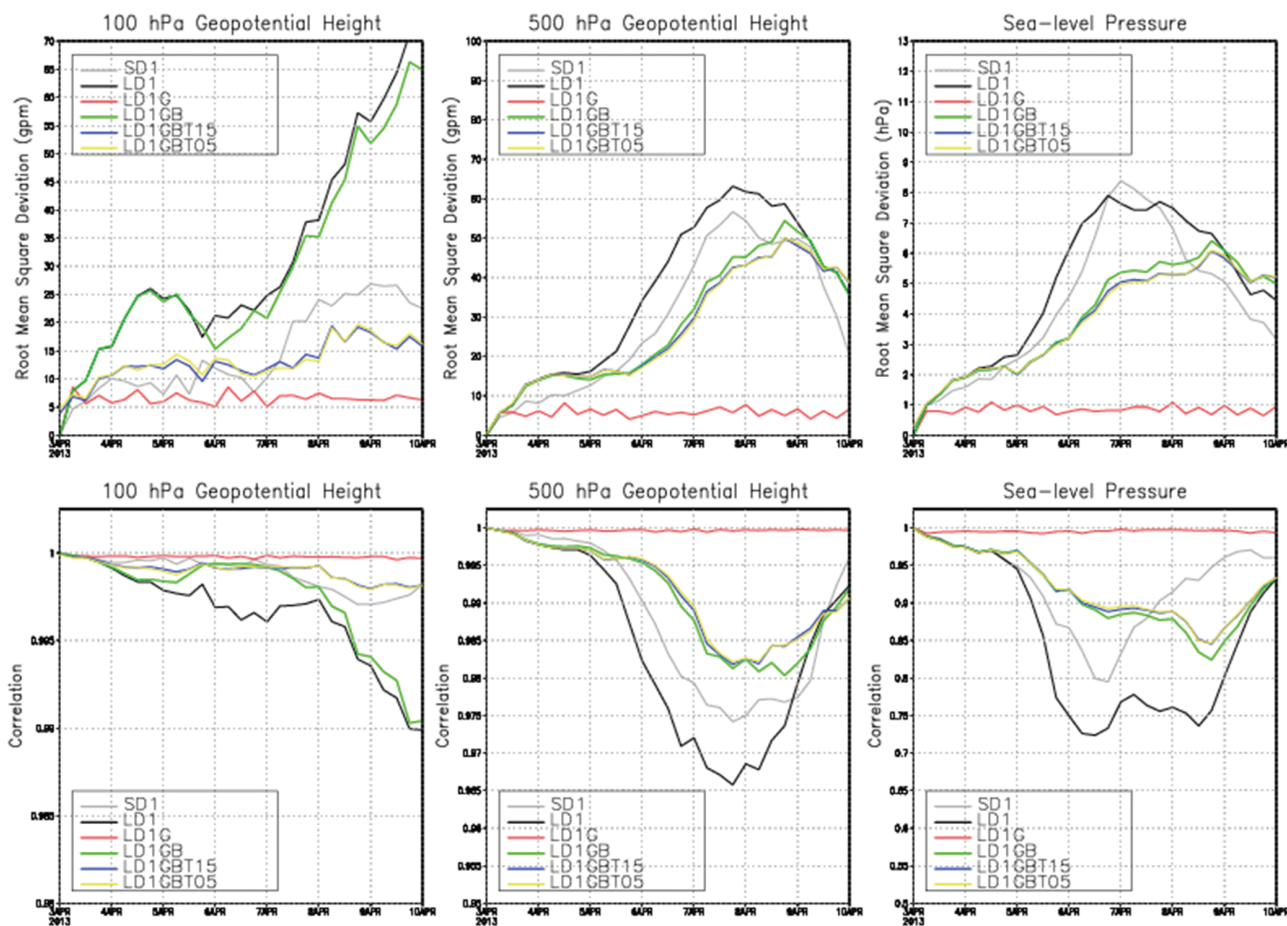


FIGURE 3 (Top) Root-mean-square deviations (RMSDs) and (bottom) correlation coefficients of (left) 100 hPa and (center) 500 hPa geopotential heights, and (right) sea-level pressure for the SD1, LD1, LD1G, LD1GB, LD1GBT15, and LD1GBT05 experiments

2011), and lack of a subgrid-scale heated-slope-induced vertical circulation (SHVC) (Chao, 2012) may also be important error sources in the vicinity of steep orographic areas. Mesoscale vortices generated in steep orographic regions around the SB in boreal summer have been of great interest due to their close connection with heavy rainfall on the downwind side (e.g., Wang & Orlanski, 1987; Zhang *et al.*, 2014). However, issues regarding topography-related errors in these areas have not received much attention.

In the WRF model, the sigma coordinate used as the terrain-following coordinate can cause PGF errors far above steep terrain regions. To examine to what extent the sigma coordinate is responsible for the low prediction quality of the LD1 experiment, we attempted to implement the hybrid-sigma coordinate in the WRF to relax the vertical coordinate surface towards isobaric surfaces at upper levels. However, these attempts did not improve the prediction accuracy (not shown), which indicates that the prediction errors initiated around the SB may be related to spurious disturbances generated at low levels, where the hybrid coordinate is similar to the pure sigma coordinate. Effects of the SHVC were also tested in the model by ventilating heat and moisture in low levels near the SB towards the top of the TP regions. However, no positive impact on the predictions for April 3, 2013 was found (not shown). The topographic wind correction and shading effects implemented in the WRF model did not improve the predictions either.

In the UTLS over northern Manchuria, our model shows cold biases as large as about -5 K over wide areas (LD1 and LD1GB in Figure 4) when compared with the ECMWF Interim data used for the initial and lateral boundary conditions of those experiments. These biases are not found in the LD1G experiment because the temperature at all grid points is nudged toward the ECMWF data. This warm layer in the UTLS over northern Manchuria (Kozubek *et al.*, 2015) can be related to the downward branch of the BD circulation in the stratosphere in winter and spring, as is revealed through ozone distributions in these seasons (Šácha *et al.*, 2015).

3.2 | Methods for error reduction

Spectral nudging was proposed to reduce erratic differences between a regional model and global analyses or forecasts (e.g., Miguez-Macho *et al.*, 2004; Omrani, Drobinski, & Dubos, 2012). Its effects have mainly been studied for regional climate simulation and downscaling issues (e.g., Gómez & Miguez-Macho, 2017; Liu *et al.*, 2012). Apart from the original purpose, in this study, we emphasize another potential role of spectral nudging in alleviating uncertainties related to model errors around steep terrain areas rather than considering the improvement of individual error sources such as the PGF term, horizontal diffusion, topographic wind correction and shading effects, or subgrid-scale thermal circulations.

Figure 3 demonstrates that spectral nudging significantly reduces model biases when the large domain 1 is used. The quasi-stationary RMSDs and correlation coefficients close to one in the LD1G experiment indicate that spectral nudging improves the model predictions by forcing the model to approach the ECMWF reanalyses. This improvement seems to be achieved by suppression of abrupt vortex motions and updrafts over steep topographic regions such as the SB through spectral nudging. More importantly, spectral nudging is also quite effective in removing noisy motions, even when it is only applied to narrow areas west of the SB illustrated by C-shaped masked areas in Figure 1 (LD1GB in Figure 3). Similar improvements are also found in wind and temperature (Figures S5 and S6). Consequently, we can see that the localized spectral nudging is useful in that it is capable of effectively reducing uncertainties related to model errors around steep topographic regions.

When compared with the LD1 experiment, improvement in the predictions at 500 hPa and sea level through the localized spectral nudging (LD1GB) is evident after about 1–2-day forecast time (Figure 3). A similar improvement is also found in the LD1GB experiment driven by the GFS forecasts for 3 April case (Figure S4). For April 3 case, the RMSDs and correlation coefficients of the 500-hPa geopotential height and sea-level pressure in the LD1GB indicate an improvement in the prediction for a forecast time period of roughly 3–5 days compared with the SD1 experiment where the TP and MK regions are not included (Figure 3). However, such an improvement in the LD1GB with respect to the SD1 is not clearly found for the other cases driven by the ECMWF reanalyses (Figure S8). In the case of April 3, the prediction errors (large RMSD and small correlation coefficients) of the LD1GB after a 5-day forecast time increase with time as fast as those of the LD1 experiment. This means that the localized spectral nudging has positive impacts in the tropospheric prediction for a forecast period of less than 5 days. However, the effect of localized spectral nudging is negligible in the UTLS. Cold biases in the UTLS over the MK region are not ameliorated in the LD1GB experiment (Figure 4).

The cold biases in the UTLS are alleviated by raising the model top to 15 hPa retaining the vertical resolution in the UTLS (LD1GBT15 in Figure 4). In regional modeling, there is no device to force downward flow associated with the BD circulation through the model top boundary. Thus, it is unlikely that these warm pool areas and related physics are properly simulated in our model as long as the model top height is too low for the model to internally and appropriately simulate meridional flows related to the BD circulation and compensating downward motions in the lower stratosphere. In fact, the comparison of LD1GBT15 with the other experiments shows that the model top of 50 hPa is not sufficient to properly simulate the warm pool areas in

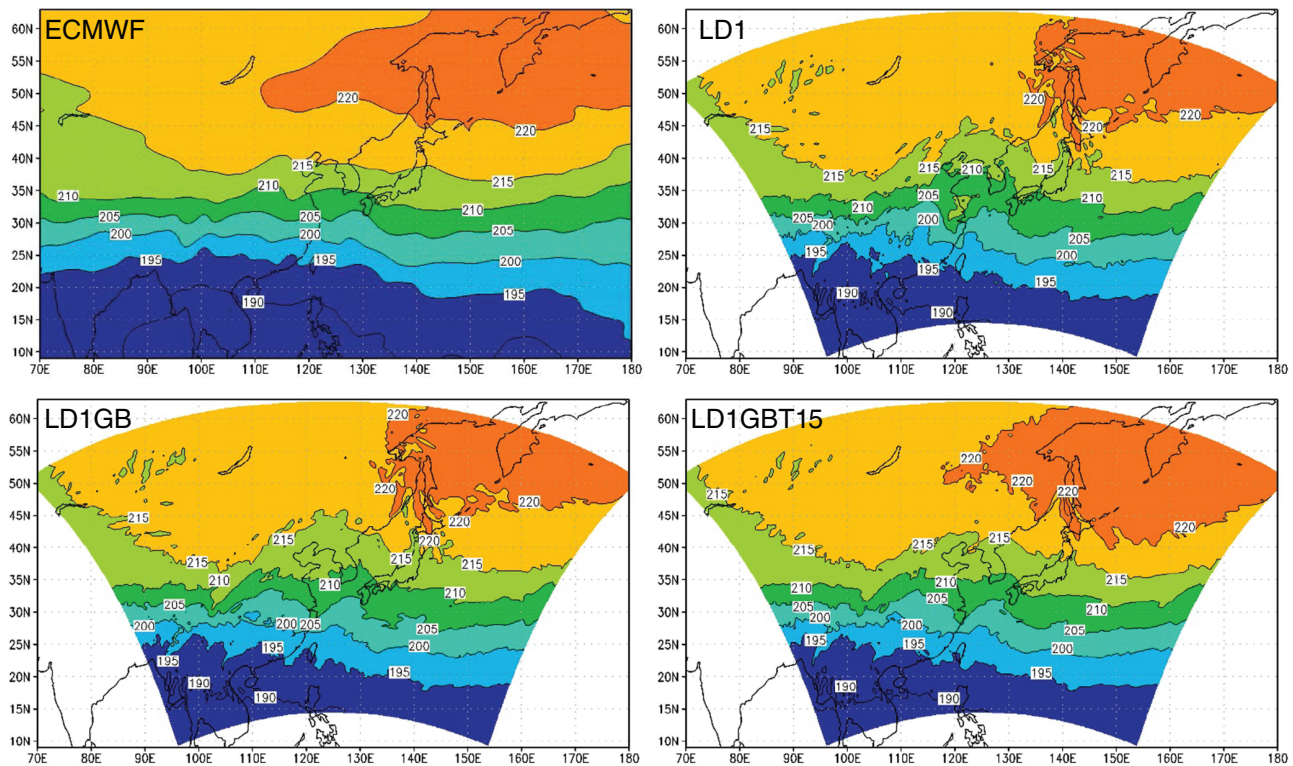


FIGURE 4 Temperature at 100 hPa and 0000 UTC on April 5, 2013 (48-hr forecast time) for the ECMWF Interim data, LD1, LD1GB, and LD1GBT15 experiments

the UTLS (Figure 4). Raising the model top to 5 hPa (LD1GBT05), however, does not further improve results compared with the LD1GBT15 experiment (see blue and yellow lines in Figure 3).

The comparison of RMSDs and correlation coefficients of the LD1GBT15 with those of the LD1GB (Figure 3) indicates that it is effective to raise the model top to achieve better regional predictions even in the troposphere as well as in lower stratosphere (100 hPa) for Northeast Asia in spring when strong vertical coupling may occur in the UTLS (e.g., Kozubek *et al.*, 2015; Šácha *et al.*, 2015). Figure 3 shows that the improvement obtained through raising the model top height mainly occurs later in the model predictions (e.g., after 4–5-day forecast time). These advantages of the high-top model for regional predictions for Northeast Asia are also found in the other cases driven by the ECMWF reanalyses (Figure S9).

4 | SUMMARY AND DISCUSSIONS

Optimized designs with respect to domain size, domain location, and model top height are required for more reliable regional weather forecasts and climate predictions. Despite large amount of studies about the impact of the domain configuration on regional predictions, optimal domain configuration for Northeast Asia has not been extensively studied.

In this study, we investigated the impact of the domain size, domain location and model top height on short- to medium-range regional predictions for Northeast Asia in spring using the WRF model.

Our numerical experiments and analysis clearly show that a horizontally extended model domain can cause significant errors in regional predictions for Northeast Asia in spring. It is found that these errors are closely related to (a) erratic vortex motions and updrafts around steep terrain regions west of the SB due to topography-related errors, and (b) cold biases in the UTLS over northern Manchuria related to the incorrect simulation of the vertical coupling with the lower stratosphere in spring when a low-top model is used. A series of numerical simulations suggests that such biases can be considerably reduced when spectral nudging is only applied to a narrow region of steep slopes west of the SB and the model top is raised to 15 hPa, retaining the vertical resolution in the UTLS. Localized spectral nudging is mainly effective in the troposphere at a forecast time period of less than 5 days and the use of the high-top model yields better predictions in both the troposphere and lower stratosphere mainly at a forecast time period beyond 4–5 days.

It has been generally accepted that the use of finer spatial resolution would help mitigate model errors. In fact, increasing computing power has enabled us to use regional or global models with finer spatial resolution. However, it is

not generally expected that model predictions for Northeast Asia are improved using finer spatial resolution because the detailed representation of the complicated topography in Northeast Asia can cause unavoidable model errors. The use of a larger horizontal domain to avoid side effects from lateral boundaries may include the complex topographic areas such as the TP. As a result, the extended model domain may lead to degradation of the prediction accuracy for Northeast Asia. Our analysis presents effective techniques to alleviate model errors and thus to improve short-to medium-range regional predictions when a horizontally extended domain is used. Our findings suggest that it is helpful to consider localized spectral nudging for steep terrain areas and a higher model top for better regional predictions. Importantly, our findings can also be applied to regional predictions in other geographic regions.

ACKNOWLEDGEMENTS

We are greatly appreciated the reviewer for spending his valuable time to read through the manuscript and to give us useful comments and suggestions on our manuscript. ECMWF Interim reanalyses are available through <https://rda.ucar.edu/datasets/ds627.0/>, and NCEP GFS forecasts can be obtained from <ftp://ftp.ncep.noaa.gov/pub/data/nccf/com/gfs/prod/>. The modeling results presented in this study are available at doi:10.22647/EAPL-MD_2013040300 and <http://eapl.yonsei.ac.kr>. This work was funded by the Korean Meteorological Industry Promotion Agency under Grant KMIPA-2015-2063 and the Korea Polar Research Institute (PN17081). I.-S.S. was supported by research fund PE17020 from Korea Polar Research Institute.

REFERENCES

- Butchart, N. (2014). The Brewer-Dobson circulation. *Reviews of Geophysics*, 52, 157–184.
- Chao, W. C. (2012). Correction of excessive precipitation over steep and high mountains in a GCM. *Journal of the Atmospheric Sciences*, 69, 1547–1561.
- Collin, J., Déqué, M., Radu, R., & Somot, S. (2010). Sensitivity study of heavy precipitation in limited area model climate simulations: Influence of the size of the domain and the use of the spectral nudging technique. *Tellus*, 62A, 591–604.
- Demirhan Bari, D., Gabriel, A., Körnich, H., & Peters, D. W. H. (2013). The effect of zonal asymmetries in the Brewer-Dobson circulation on ozone and water vapor distributions in the northern middle atmosphere. *Journal of Geophysical Research: Atmosphere*, 118, 3447–3466.
- Giorgi, F., & Mearns, L. O. (1999). Introduction to special section: Regional climate modeling revisited. *Journal of Geophysical Research*, 104, 6335–6352.
- Goméz, B., & Míguez-Macho, G. (2017). The impact of wave number selection and spin-up time in spectral nudging. *Quarterly Journal of the Royal Meteorological Society*, 143, 1772–1786.
- Good, B., Gadian, A., Lock, S. J., & Ross, A. (2014). Performance of the cut-cell method of representing orography in idealized simulations. *Atmospheric Science Letters*, 15, 44–49.
- Jiang, X., Li, Y., Zhao, X., & Koike, T. (2012). Characteristics of the summertime boundary layer and atmospheric vertical structure over the Sichuan basin. *Journal of the Meteorological Society of Japan*, 90C, 33–54.
- Jiménez, P. A., & Dudhia, J. (2012). Improving the representation of resolved and unresolved topographic effects on surface wind in the WRF model. *Journal of the Applied Meteorology and Climatology*, 51, 300–316.
- Jones, R. G., Murphy, J. M., & Noguera, M. (1995). Simulation of climate change over Europe using a nested regional-climate model. I: Assessment of control climate, including sensitivity to location of lateral boundaries. *Quarterly Journal of the Royal Meteorological Society*, 121, 1413–1449.
- Kozubek, M., Krizan, P., & Lastovicka, J. (2015). Northern hemisphere stratosphere winds in higher midlatitudes: Longitudinal distribution and long-term trends. *Atmospheric Chemistry and Physics*, 15, 2203–2213.
- Landman, W. A., Seth, A., & Camargo, S. J. (2005). The effect of regional climate model domain choice on the simulation of tropical cyclone-like vortices in the Southwestern Indian Ocean. *Journal of Climate*, 18, 1263–1274.
- Leduc, M., & Laprise, R. (2009). Regional climate model sensitivity to domain size. *Climate Dynamics*, 32, 833–854.
- Lee, J., & Hong, J. (2016). Implementation of spaceborne lidar-retrieved canopy height in the WRF model. *Journal of Geophysical Research: Atmosphere*, 121, 6863–6876.
- Lee, J., Shin, H. H., Hong, S. Y., Jiménez, P. A., Dudhia, J., & Hong, J. (2015). Impacts of subgrid-scale orography parameterization on simulated surface layer wind and monsoonal precipitation in the high-resolution WRF model. *Journal of Geophysical Research*, 120, 644–653.
- Liu, P., Tsipiridi, A. P., Hu, Y., Stone, B., Russell, A. G., & Nenes, A. (2012). Differences between downscaling with spectral and grid nudging using WRF. *Atmospheric Chemistry and Physics*, 12, 3601–3610.
- Mahrer, Y. (1984). An improved numerical approximation of the horizontal gradients in a terrain-following coordinate system. *Monthly Weather Review*, 112, 918–922.
- Messinger, F. (1982). On the convergence and error problems of the calculation of the pressure gradient force in sigma coordinate models. *Geophysical and Astrophysical Fluid Dynamics*, 19, 105–117.
- Míguez-Macho, G., Stenchikov, G. L., & Robock, A. (2004). Spectral nudging to eliminate the effects of domain position and geometry in regional climate model simulations. *Journal of Geophysical Research*, 109, D13104.
- Omrani, H., Drobinski, P., & Dubos, T. (2012). Spectral nudging in regional climate modeling: How strongly should we nudge? *Quarterly Journal of the Royal Meteorological Society*, 138, 1808–1813.
- Park, S. H., Klemp, J. B., & Skamarock, W. C. (2014). A comparison of mesh refinement in the global MPAS-A and WRF models using an idealized normal-mode baroclinic wave simulation. *Monthly Weather Review*, 142, 3614–3634.
- Ruiz-Arias, J. A., Pozo-Vázquez, D., Lara-Fanego, V., Santos-Alamillos, F. J., & Tovar-Pescador, J. (2011). A high-resolution topographic correction method for clear-sky solar irradiance derived with a numerical weather prediction model. *Journal of Applied Meteorology and Climatology*, 50, 2460–2472.
- Šácha, P., Kuchař, A., Jacobi, C., & Piscořt, P. (2015). Enhanced internal gravity wave activity and breaking over the northeastern Pacific-eastern Asian region. *Atmospheric Chemistry and Physics*, 15, 13097–13112.
- Shin, U., & Lee, T. (2015). Origin, evolution and structure of meso- α -scale lows associated with cloud clusters and heavy rainfall over the Korean peninsula. *Asia-Pacific Journal of Atmospheric Sciences*, 51, 259–274.
- Simmons, A. J., & Burridge, D. M. (1981). An energy and angular-momentum conserving vertical finite-difference scheme and hybrid vertical coordinates. *Monthly Weather Review*, 109, 758–766.
- Skamarock, W. C., Klemp, J. B., Dudhia, J., Gill, D. O., Baker, D. M., Duda, M. G., ... Powers, J. G. (2008). A description of the advanced research WRF version 3. NCAR/TN-475+STR.
- Tao, S., & Ding, Y. (1981). Observational evidence of the influence of the Qinghai-Xizang (Tibet) Plateau on the occurrence of heavy rain and severe convective storms in China. *Bulletin of the American Meteorological Society*, 62, 23–30.
- Vannitsem, S., & Chomé, F. (2005). One-way nested regional climate simulations and domain size. *Journal of Climate*, 18, 229–233.
- Wang, B., & Orlanski, I. (1987). Study of a heavy rain vortex formed over the eastern flank of the Tibetan Plateau. *Monthly Weather Review*, 115, 1370–1393.
- Warner, T. T., Peterson, R. A., & Treadon, R. E. (1997). A tutorial on lateral boundary conditions as a basic and potentially serious limitation to regional numerical weather prediction. *Bulletin of the American Meteorological Society*, 78, 2599–2617.

Zhang, P., Li, G., Fu, X., Liu, Y., & Li, L. (2014). Clustering of Tibetan Plateau vortices by 10–30 day intraseasonal oscillation. *Monthly Weather Review*, *142*, 290–300.

SUPPORTING INFORMATION

Additional Supporting Information may be found online in the supporting information tab for this article.

How to cite this article: Song I-S, Byun U-Y, Hong J, Park S-H. Domain-size and top-height dependence in regional predictions for the Northeast Asia in spring. *Atmos. Sci. Lett.* 2018;19:e799. <https://doi.org/10.1002/asl.799>